RSC Advances

This is an *Accepted Manuscript*, which has been through the Royal Society of Chemistry peer review process and has been accepted for publication.

Accepted Manuscripts are published online shortly after acceptance, before technical editing, formatting and proof reading. Using this free service, authors can make their results available to the community, in citable form, before we publish the edited article. This *Accepted Manuscript* will be replaced by the edited, formatted and paginated article as soon as this is available.

You can find more information about *Accepted Manuscripts* in the Information for Authors.

Please note that technical editing may introduce minor changes to the text and/or graphics, which may alter content. The journal's standard Terms & Conditions and the Ethical guidelines still apply. In no event shall the Royal Society of Chemistry be held responsible for any errors or omissions in this *Accepted Manuscript* or any consequences arising from the use of any information it contains.

ROYAL SOCIETY OF CHEMISTRY

www.rsc.org/advances

Journal Name

RSCPublishing

COMMUNICATION

Effect of graphene and carbon nanotubes in the negative active materials of lead acid batteries operating under high-rate partial-state-of-charge operation.

Cite this: DOI: 10.1039/x0xx00000x

Received ooth January 2012,
Accepted ooth January 2012

DOI: 10.1039/x0xx00000x

www.rsc.org/

S. Mithin Kumar, S. Ambalavanan and Sundar Mayavan*

Consequences of including graphene and carbon nanotubes in the negative plates of lead acid battery have been investigated after exposure to high rate partial state of charge duty cycle.

The unrelenting issues associated with fossil fuels (like high cost, limited reserve, carbon dioxide emissions) have encouraged the development of range of hybrid electric vehicles (start-stop hybrid, power-assist hybrid and full hybrid) for transport applications. Lead acid batteries (LAB) in hybrid electric vehicle typically operate under high rate partial state of charge (HRPSoC). This operating mode is quite challenging as it involves short duration of charge and discharge with high current rates. The regular LAB operating under this mode suffer (or fails prematurely) from two major issues, namely low charge acceptance and progressive sulfation of negative active material (NAM). Creating hybrids/composites structures involving NAM is highly essential to create innovative and intriguing materials as pristine NAM alone cannot satisfy requirements of LAB operating under HRPSoC.

Carbon addition (to NAM) is considered to be the best strategy to create new functionalities to overcome the mechanism responsible for progressive sulfation. Moseley has explained the possible function of carbon in NAM under HRPSoC conditions.[1] Carbon particles improve the electronic conductivity of NAM by forming conductive network between lead sulfate crystals. Presence of carbon may impede the progressive growth of lead sulfate crystals. The capacitive element of carbon can support charge and discharge events at high rates.[2] Different types of carbon (with different properties) give rise to different results when added to NAM, some are advantageous and some has no effect.[3-5] Hence, active research is currently devoted towards finding an ideal additive for NAM under HRPSoC condition. In this regard, nanostructured graphitic carbon materials offer great promise because of their unusual properties. However, their utilization as NAM additives for LAB operating under HRPSoC condition are rarely studied. Recently, our group found that LAB performance under HRPSoC condition can be improved by replacing conventional carbon black with multiwalled carbon nanotube (MWNT) conductive additive.[6] MWNT additives increase the electric conductivity of active mass with sufficient percolation network.

Graphene, a basic building block in all graphitic materials, is a relatively new and exciting material, exhibiting unique electronic, mechanical, and chemical properties.[7,8] Recently, graphene has been used as a conductive additive for lithium ion battery cathode materials.[9,10] Graphene nanosheets form electron conducting path/ network within the cathode thereby improving the capacity and cyclability. In this study we examine the prospects of graphene incorporation (as a conductive additive) into NAM to meet HRPSoC demands. The performance of graphene incorporated in NAM was compared with both single walled carbon nanotube (SWNT) and MWNT incorporated NAM. This study is of great significance as it will allow us to identify the structural changes and elementary process that takes place at the negative plates under HRPSoC cycling and evaluates which types of nano-structured carbon is ideal additive for NAM under our experimental conditions.

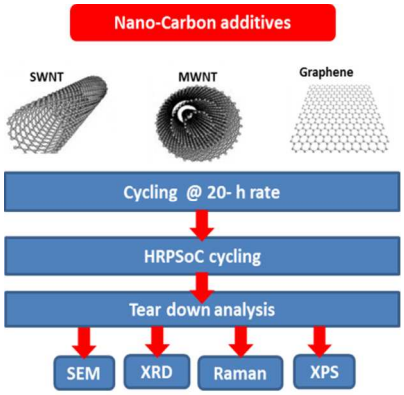

Scheme 1: Summary of additives added to NAM used in this study and the type of tests performed.

RSC Advances Accepted Manuscript

Additive	Supplier	Ave. Length	Size	Purity	Surface area
SWNT	Nano shell, USA	3-8 µm	1-2 nm (diameter)	> 98%	350-450 m^2/g
MWNT	SRL, India	5-15 µm	40-50 nm (diameter)	> 99%	-
Graphene	Nano shell, USA	1-10 µm	0.5-0.6 nm (thickness)	>99.9%	250 m^2/gm

Table 1. Characteristics (as specified by the supplier) of the nano-carbon materials used as additive to NAM in the present study.

In order to evaluate the consequences of including graphene and carbon nanotubes in NAM of LAB during HRPSoC cycling, Lead acid test cells (2 V/1.22 Ah) were assembled comprising one negative and two positive plates using lead-selenium alloy. The concentration of carbon materials (without any pre-treatment) used as additives in this study is 0.25 % by weight. Figure S1 shows the TEM image of pristine graphene, SWNT and MWNT. Dimensions of negative and positive plates were 40mm X 49 mm X 1.5 mm and 40 mm X 49 mm X 2.0 mm respectively. The negative lead paste was prepared by conventional method and assembled with PVC separator. The performance of the cells was limited by the negative plate. Firstly, the assembled cells were subjected to 20 h rate cycling (10 cycles) at room temperature. Secondly, the cell performance was evaluated under simulated HRPSoC conditions, using a simplified profile imitating micro-hybrid driving mode.[11,12] The cells were subjected to cycling according to the following schedule. Charge at 2 C rate for 60 s, rest for 10 s, discharge at 2 C rate for 60 s, rest for 10 s. The test was stopped when the end voltage reaches 1.83 V or when the upper voltage limit of 2.83 V was

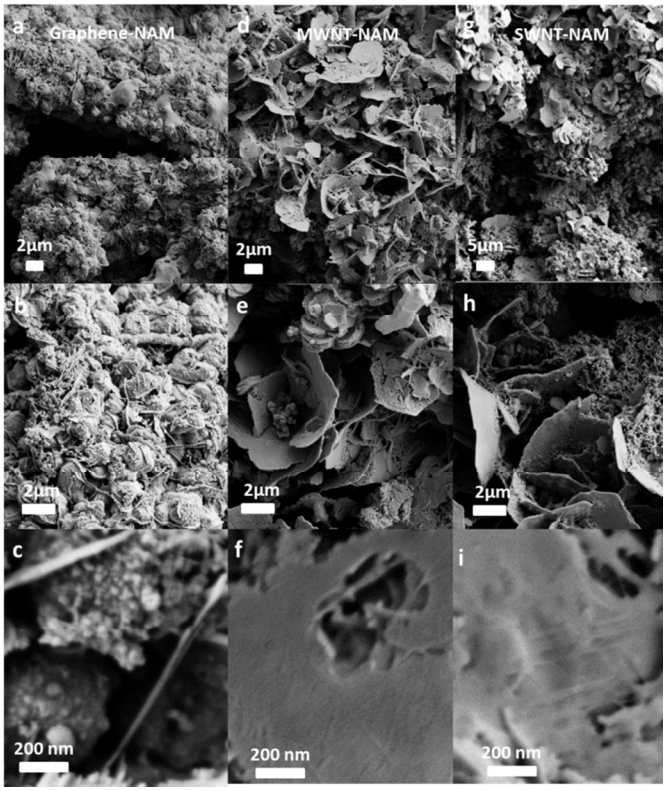

Figure 1: FE-SEM image of formed NAM (a,b,c) Graphene, (d,e,f) MWNT and (g,h,i) SWNT

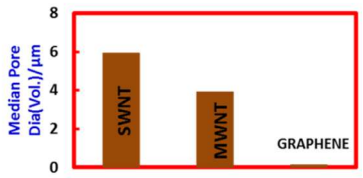

Figure 2. Porometric data for NAM with graphene, SWNT and MWNT additives

reached. The above-described cycling steps comprise of one cycle-set of the test. After this cycle set, the cell was fully re-charged (to 100% SoC) and their C20 capacity was measured then followed to second cycle-set. The charge–discharge tests were carried out using Bitrode life cycle tester. Table 1 and Scheme 1 presents a summary of NAM prepared with three nano-structured carbons and the types of tests and analyses performed within this study.

Fig. 1 shows the FE-SEM images of as-prepared NAM (before cycling) with graphene, SWNT and MWNT additives. Microstructural characterization of graphene-NAM (Figure 1a-c) reveals globular morphology (spherical) with size of aggregates 1-2 microns. Figure d-f and g-i shows that SWNT and MWNT form a network wiring in the NAM. Both SWNT and MWNT were also found to adsorb on the surface of NAM (as seen in Fig. 1f and i). From FE-SEM images it is obvious that graphene and CNTs have different impact on the structural characteristics of the negative active mass. Fig. 2 illustrates the changes in pore radius of NAM with three nano-structured carbon additives (measured by mercury porosimeter). Adding SWNT and MWNT, causes formation of large pores in NAM (2.9 µm and 2.1 µm pore radius, respectively.). Addition of graphene reduces the median pore radius to 0.26 µm i.e. negative active mass acquires membrane-sized pore structure as compared to NAM containing SWNT and MWNT. The changes in carbon type in NAM clearly reflect in changes in pore radius distribution.

Figure 3a shows the comparative cycling performance for cells with graphene, MWNT and SWNT NAM at 20h rate. Irrespective of type of carbon, the cell capacity decreases during initial cycles and then stabilizes. At the end of 10 cycles, graphene capacity (1.55 Ah) is higher as compared to SWNT (1.45 Ah) and MWNT (1.4 Ah). The cells are then subjected to HRPSoC cycling. Figure 3b shows the number of completed cycles per cycle-set for three different carbons. The total numbers of completed HRPSoC cycles depend strongly on the nature of carbons. MWNT has completed 7 consecutive cycle-sets with 41,491 cycles as against SWNT and graphene. SWNT failed after 5 consecutive cycle-sets with 26,644 cycles whereas graphene failed pre-maturely after two consecutive cycle-set with 3,874 cycles. Figure 3c shows the behaviour of the cell capacity (at C20) after each

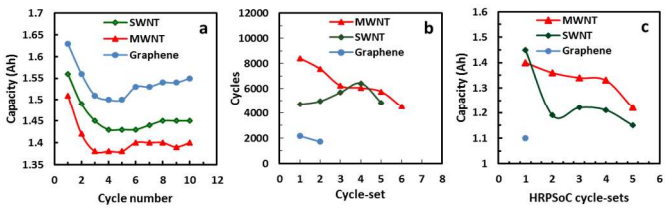

Figure 3. Comparative cycling performance of graphene, SWNT and MWNT added cell. (b) Completed HRPSoC cycles per set for cells with graphene, SWNT and MWNT. (c) Cell capacity after each HRPSoC cycle set

RSC Advances Accepted Manuscript

This journal is © The Royal Society of Chemistry 2012

Figure 4. FE-SEM image of cycled NAM (after cell failure) with (a,b,c) Graphene, (d,e,f) MWNT and (g,h,i) SWNT.

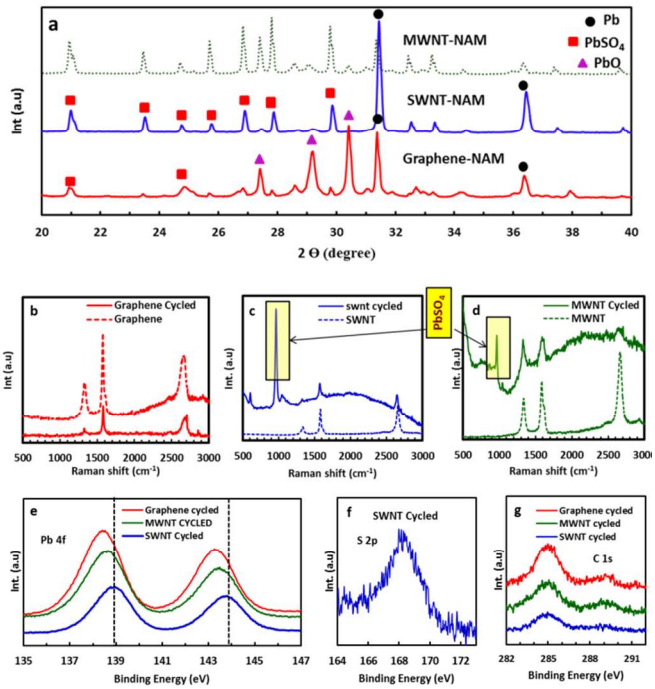

Figure 5. (a) XRD spectra of cycled NAM; (b, c, d) Raman spectroscopy of cycled NAM; (e) High resolution Pb 4f spectra of cycled NAM; (f) High resolution S 2p spectra of cycled NAM (g) High resolution C 1S spectra of cycled NAM.

HRPSoC cycle test, the capacity of cells with graphene and SWNT in NAM has decreased dramatically. The cell with MWNT-NAM shows a relatively small decrease in discharge capacity as compared to the initial capacity. These data show that the performance of MWNT-NAM is much better than SWNT and graphene based NAM cell under HRPSoC cycling.

Failed test cells (containing graphene, MWNT and SWNT) were cut open for analysis. The negative plates were taken out of the cells, washed and dried. Samples were analysed by FE-SEM, XRD, Raman spectroscopy and X-ray photoelectron spectroscopy (XPS). The FE-SEM image of MWNT/SWNT-NAM clearly reveals the distribution of unconverted lead sulfate ($PbSO_4$) crystals. $PbSO_4$ formed on the surface progressively accumulates in the negative plates, which lead to the formation of coarse crystals of irreversible lead sulphate (as shown in Fig.4 e,f,g,h,I,j. SWNT/MWNT which was firmly adsorbed onto the surface of NAM (before cycling, as seen in Fig. 1f,i) was found to detach itself from the NAM with the formation of coarse $PbSO_4$ crystals. Upon cycling, NAM undergoes large volume change (about 120 %), this volume change can result in the detachment of SWNT/MWNT, losing its efficient electronic contact with the NAM. Once SWNT/MWNT is detached, the process of converting $PbSO_4$ to Pb becomes increasingly difficult and may lead to progressive sulfation. Chemical composition and phases present on the electrode surfaces was analysed by XRD (Fig. 5a). XRD data indicates the formation of $PbSO_4$ diffraction peaks along with lead peak in case of MWNT and SWNT.[2] This is an indication that MWNT/SWNT-NAM is sulphated more in HRPSoC condition. Interestingly, for graphene-NAM lead oxide (PbO) crystals are formed instead of $PbSO_4$. FE-SEM image (Fig. 4 a,b,c) shows the presence of leaf-like crystals (all over the surface) which is indicative of the presence of PbO crystal and impedes significantly the reaction of lead oxidation. XRD confirms the presence of considerable amounts of PbO along with small amount of $PbSO_4$. The diffraction peaks for PbO are higher than that of metallic lead, which indicates that a thick PbO layer has formed. The formation of PbO (or conversion of Pb to PbO) under HRPSoC duty cycle may be the reason for pre-mature failure of the cell. Figure 5 b,c,d shows the Raman spectroscopy of MWNT, SWNT and graphene based NAM. All samples display prominent bands at around 1300, 1600 and 2700 cm^{-1}, which corresponds to D, G and 2D band of graphitic materials, respectively.[13] The intensity ratio of the D to G bands (I_D/I_G ratio, which is a measure of the degree of disorder (or defect density)) of NAM-Graphene decreases. The presence of H_2SO_4 (under test condition) may facilitate the conversion of sp^3 to sp^2 graphitic carbon[14] (removal of defects) and hence the decrease. In addition, NAM with both SWNT and MWNT show an additional peak at 978 cm^{-1}. The Raman peak at 978 cm^{-1} is assigned to the symmetric stretching vibrational mode of the sulfate group in $PbSO_4$.[15] But NAM with graphene does not show any peak relating to $PbSO_4$. Fig. 5e compares the Pb 4f peaks of NAM with graphene, SWNT and MWNT. The Pb 4f spectra of graphene-NAM shows two broad singlet peaks corresponding to Pb 4f7/2 and Pb 4f5/2 centered around binding energy values 138.5 eV and 143 eV respectively. No sulphur peak is evident. This indicates that majority of lead appears to be present as lead oxide. In case of SWNT a clear blue shift in peak is observed which indicates the presence of lead as lead sulfate. In addition the sample show S 2p peak at 168.5 eV (Figure 5f) which is assigned to

RSC Advances Accepted Manuscript

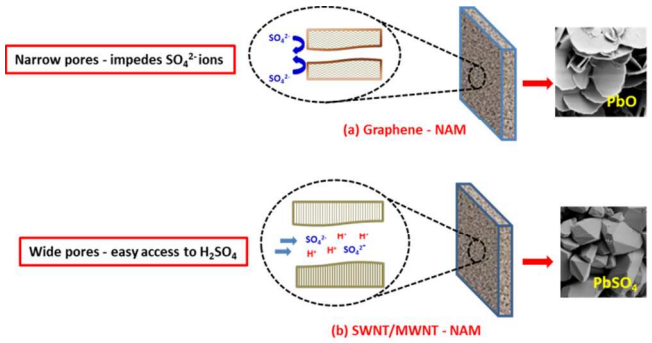

Scheme 2. Model scheme for the PbO and $PbSO_4$ formation in NAM pores with graphene and SNT/MWNT, respectively.

sulphur species present in $PbSO_4$.[16] The Figure 5g shows the C 1s peak of NAM with three different carbon additives. All samples show a major peak at 285.2 eV with a small shoulder at 289 eV. According to literature the peak at 285.2 eV correspond to carbon attached to hydrogen atom (C-H; BE = 285.2 eV).[17,18] The formation of C-H species indicates attachment of hydrogen to the C-C π-bonds resulting in C-H bond formation during HRPSoC cycling. In the present case, C-H formation may be due to intercalation/adsorption of H^+ ions (from electrolyte H_2SO_4). It has been well documented that it is possible to form local C-H bonds by chemical interaction between hydrogen and SWNT/MWNT/ Graphene.[19,20] The small shoulder at 289.6eV can be assigned to C=O in carboxylic acid, ester and lactone functionalities.[21] The formation of C=O may be due to oxidation of carbon under acidic conditions and also by oxygen from positive plate (see supporting information).[22]

XPS, XRD and Raman data clearly suggest the formation of $PbSO_4$ and PbO/OH phases in case of SWNT-NAM and graphene/MWNT-NAM, respectively. Pavlov et al[2] had studied the formation of PbO in H_2SO_4, and has explained the mechanism for the formation of PbO in NAM using porometric data. NAM with narrow pores (less than 1.0 mm) acts as a semi-permeable membrane for ionic transport, since SO_4^{2-} and HSO_4^- ions are relatively big in size and less mobile, their movement through small pores may be impeded and pores are filled only with water. Water dissociation and H^+ ion migration leaves OH^- ions (in pores), and thus increase the pH of the pore solution to alkaline values. A reaction between Pb^{2+} and OH^- ions starts, producing $Pb(OH)_2$ and PbO. Thus, PbO is formed despite active lead is in contact with H_2SO_4.

We observed a similar trend toward formation of PbO in our present study. Scheme 2 illustrates the process leading to formation of PbO in graphene-NAM. Our porometric data give pore radius values of 2.9 µm, 2.1 µm and 0.26 µm for NAM with SWNT, MWNT and graphene, respectively. NAM- graphene with narrow pores may act as a semi-permeable membrane and blocks/impedes the movement of large size SO_42- and HSO_4- ions into pores. Thus the solution inside pores becomes alkaline resulting in the formation of PbO. Moreover, wide variety of species can be intercalated between graphene sheets[1,18,19] and hence the intercalation of ions $(H^+)/(HSO_4^-)$ and molecules (H_2SO_4) is also possible (impeding the interaction of NAM with H_2SO_4).

Conclusions

This study allowed us to identify the elementary process that take place at the negative plates on HRPSoC cycling. Graphene and CNTs have different impact on the structural and electrochemical properties of NAM. Under HRPSoC cycling, MWNT shows much better activity and performance than SWNT and graphene based NAM. For SWNT-NAM, the dominating elementary process is the formation of $PbSO_4$ on the electrode surface. But for graphene-NAM, the dominating elementary process is the formation of PbO on the electrode surface (which impedes significantly the reaction of lead oxidation and results in pre-mature cell failure as compared to SWNT and MWNT).

Notes and references

CSIR-Central Electrochemical Research Institute, Karaikudi, India
914565241453; sundarmayavan@cecri.res.in

† Electronic Supplementary Information (ESI) available: TEM image, Experimental and instrumentation. See DOI: 10.1039/c000000x/

1 P.T. Moseley, J. Power Sources, 2009, **191**, 134.
2 D. Pavlov and P. Nikolov, J. Power Sources, 2013, **242**, 380.
3 K. Nakamura, M. Shiomi, K. Takahashi and M. Tsubota, *J. Power Sources*, 1996, **59**, 153.
4 M. Shiomi, T. Funato, K. Nakamura, K. Takahashi and M. Tsubota, *J. Power Sources*, 1997, **64**, 147.
5 D. Pavlov, P. Nikolov and T. Rogachev, *J. Power Sources*, 2011, **196** 5155
6 M. Saravanan, P. Sennu, M. Ganesan and S. Ambalavanan, *J. Electrochem. Soc.* 2013, **160**, A70
7 D. Wei and Y. Liu, *Adv. Mater.*, 2010, **22**, 3225
8 C. N. R. Rao, A. K. Sood, K. S. Subrahmanyam and A. Govindaraj, *Angew. Chem., Int. Ed.*, 2010, **48**, 7752
9 G. Kucinskis, G. Bajars and J. Kleperis, *J. Power Sources*, 2013, **240**, 66
10 C. Su, X. Bu, L. Xu, J. Liu and C. Zhang, *Electrochim. Acta*, 2012, **64**, 190
11 D. Pavlov, P. Nikolov, and T. Rogachev, *J. Power Sources*, 2010, **195**, 4444
12 D. P. Boden, D. V. Loosemore, M. A. Spence, and T. D. Wojcinski, *J. Power Sources*, 2010, **195**, 4470
13 S. Mayavan, J. B Sim and S. M Choi, *J. Mater. Chem*., 2012, **22**, 6953
14 W. Gao, L. B. Alemany, L. Ci and P. M. Ajayan, *Nature Chemisty,* 2009, **1**, 403
15 N. Dupuy and Y. Batonneau, *Analytica Chimica Acta*, 2003, **495**, 205
16 S. Mayavan, H-S Jang, M-J Lee, S H Choi and S-M Choi, *J. Mater. Chem. A*, 2013, **1**, 3489
17 M. J. Webb, P. Palmgren, P. Pal, O. Karis and H. Grennberg, *Carbon*, 2011, **49**, 3242
18 M. L. Ng, R. Balog, L. Hornekær, A. B. Preobrajenski, N. A. Vinogradov, N. Mårtensson and K. Schulte, *J. Phys. Chem. C*, 2010, **114**, 18559
19 V. Tozzini and V. Pellegrini, *Phys. Chem. Chem. Phys*., 2013, **15**, 80
20 A. Nikitin, X. Li, Z. Zhang, H. Ogasawara, H. Dai and A. Nilsson, 2008, *Nano Lett*., **8**, 162
21 Y. Wang, X. Tong, X. Guo, Y. Wang, G. Jin and X. Guo, *Nanotechnology*, 2013, **24**, 475602
22 K. R. Bullock, *J Power Sources*, 2010, **195**, 4513

RSC Advances Accepted Manuscript

This journal is © The Royal Society of Chemistry 2012

Table of contents

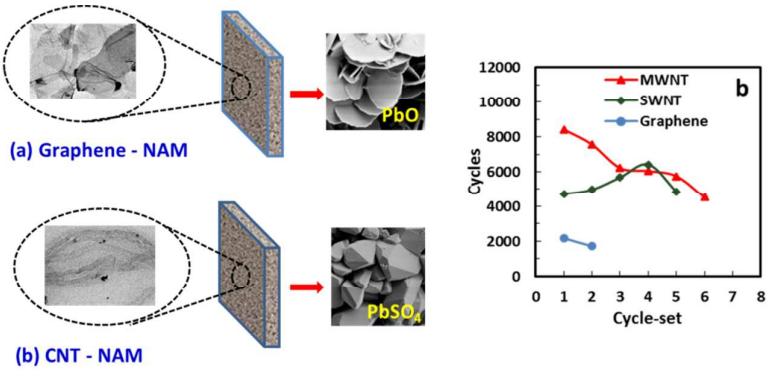

Graphene and CNTs have different impact on the structural and electrochemical properties of lead acid battery NAM under HRPSoC cycling.

RSC Advances Accepted Manuscript